AIAA JOURNAL
Vol. 43, No. 7, July 2005

Flow Around an Object Projected from a Cavity into a Supersonic Freestream

Scott T. Bjorge* and Mark F. Reeder†
U.S. Air Force Institute of Technology, Wright–Patterson Air Force Base, Ohio 45433-7765
C. Subramanian‡
Florida Institute of Technology, Melbourne, Florida 32901-6975
and
Jim Crafton§ and Sergey Fonov§
Innovative Scientific Solutions, Inc., Dayton, Ohio 45440

Store–cavity interaction was investigated by using fast-response pressure transducers, high-speed schlieren photography, and pressure-sensitive paint (PSP) at freestream Mach numbers of 1.8 and 2.9. The influence of Mach number on the interaction of a cavity ($L/D = 3.6$, $W/D = 3.8$) and a modeled store was characterized. High-speed schlieren photography illustrated the real-time motion of coherent spanwise structures in the Mach 1.8 flow and revealed the absence of these structures in the Mach 2.9 flow. The spectra measured in the Mach 1.8 flow exhibited clear resonant peaks consistent with Rossiter modes, whereas the Mach 2.9 flow did not. The mean floor pressure increased as the store was positioned nearer to the free shear layer for both Mach number conditions. Interestingly, the level of the pressure fluctuations measured on the cavity floor decreased for the Mach 1.8 case when the store was positioned in the freestream but increased for the Mach 2.9 case. PSP was applied to the cavity floor and to the modeled store. Integration of the measured pressure field on the store yielded information on the forces and pitching moment. Schlieren imaging of a modeled store exiting the cavity indicated that the free shear layer is slightly displaced by the moving store.

Introduction

INTERNAL weapons carriages have a number of design advantages in comparison to external stores, including, but not limited to, reduced aerodynamic drag and lower radar cross section. However, there are a few serious impediments to this approach, particularly when release at supersonic speeds is required. The resonance generated by air moving past the cavity under this condition may lead to deterioration of weapon electronics and structural fatigue. A second, very serious difficulty is that the unsteady aerodynamics accompanying store separation from the weapons bay can lead to unpredictable motion of the store. A number of studies are underway to alleviate these concerns in both areas.[1,2]

A greatly simplified description of resonant tone generation within the cavity is as follows. A Kelvin–Helmholtz (K–H) instability initiates a discrete spanwise vortex sheet at the leading edge of the cavity. As the vortex convects downstream, it grows and evolves until it reaches the trailing edge of the cavity, whereupon it interacts with the trailing edge of the cavity and a pressure wave convects upstream through the subsonic flow within the cavity. This pressure wave stimulates the formation of another K–H vortex and the self-sustaining cycle, termed cavity resonance, is repeated. The resonant cavity falls in the came category of other fluid-resonant phenomena, one example of which is the screech tone generated by an underexpanded supersonic jet. A number of factors influence the resonance phenomena, including cavity geometry, vortex interaction, and flow properties. A more complete and general description of cavity flows is given by Rockwell and Naudascher,[3] among others.

The effect of compressibility on the cavity flow dynamics has been addressed in a number of fairly recent studies. Zhang and Edwards[4] reported that, for a given cavity dimension, a cavity of a given L/D produces a higher level of fluctuation for a Mach 1.5 freestream than for a Mach 2.5 freestream. They investigated a variety of length-to-depth ratios and found that a transition from a relatively weak transverse oscillation to a relatively strong longitudinal oscillation occurs as L/D is increased from one to three. The standard deviation of the pressure normalized by the dynamic pressure of the freestream is a factor of three to four times higher for a Mach 1.5 freestream than for a Mach 2.5 freestream between $L/D = 3$ and 5. However, they do report that the Mach 2.5 freestream leads to dominant modes.

Murray and Elliott[5] utilized schlieren photography and laser sheet lighting to study cavity flow for freestream conditions ranging from Mach 1.8 to 3.5. Using the latter, they clearly illustrated the decreased coherence of spanwise flow structures as the freestream Mach number was increased from 1.8 to 3.5. They also report that the convective velocity of the dominant structures was accurately estimated by 0.57 times the freestream velocity.

Unalmis et al.[6] have reported results of a study of Mach 5 flow over a cavity for $L/D = 3$ and using fast-response pressure transducers and laser sheet lighting. No evidence for coherent structures, typically induced by cavity acoustics at lower Mach numbers, was observed. Furthermore, they reported substantially less coupling between the cavity pressure fluctuations and the shear-layer fluid dynamics as compared to similar flows with lower freestream Mach numbers. Last, they report that shock impingement on the trailing edge of the cavity are aperiodic for their conditions studied.

These recent studies generally correspond well with that of Heller et al.[7] In a study of a cavity with L/D ranging from four to seven and

Presented as Paper 2004-1253 at the AIAA 42nd Aerospace Sciences Meeting, Reno, NV, 4–8 January 2004; received 19 May 2004; revision received 25 October 2004; accepted for publication 24 November 2004.

*Graduate Student; currently Captain, Aeronautical Engineer, U.S. Air Force Research Laboratory/VASM. Member AIAA.
†Assistant Professor, Department of Aeronautics and Astronautics; mark.reeder@afit.edu. Senior Member AIAA.
‡Professor of Mechanical and Aerospace Engineering. Associate Fellow AIAA.
§Research Scientist, Research and Development Department. Member AIAA.

Mach numbers ranging from 0.8 to 3.0, they used a variable density wind tunnel to show that the fluctuation level is very sensitive to the state of the incoming boundary layer in highly compressible flow environments. They measured a normalized spectral peak nearly 30 dB higher for a laminar boundary layer compared to a turbulent boundary layer for a Mach 3 freestream. This was not the case for lower Mach number values where the state of the incoming boundary layer had little, if any, affect on the pressure spectra.

Largely because of the potential deterioration of store electronics, considerable effort has been directed toward suppressing the strong pressure fluctuations in cavities through passive and active flow control. A recent comprehensive review of flow control in a cavity flow environment is given by Cattafesta et al.[1]

Flow in and around a weapons bay is approached from a different perspective by munitions experts concerned with the trajectory of a store as it is released. From this point of view, the highest priority is that the store separates cleanly from the aircraft and that its trajectory be predictable and controllable. In such an approach, the mixing layer is often modeled as a steady flow region where the air velocity increases from a region within the cavity to the freestream.[8] A time-dependent study of external store separation by Mosbarger and King[9] lends credence to the general approach. However, given the resonant cavity phenomena, one might expect the fluctuations in flow properties to play a more prominent role in the free shear layer proximate to a cavity. Even minor variations in the store's initial trajectory could lead to unpredictability in the ultimate trajectory of the store. It is conceivable that acoustic suppression could improve the predictability of store trajectory.

Computational fluid dynamics tools have also been applied to cavity flow problems. Baysal et al.[10] published findings of a computational study utilizing a Reynolds averaging turbulence model to model a flow about a store–cavity combination where the store was placed alternatively within or wholly outside the cavity. More recently, Rizzetta and Visbal[11] utilized a high-order numerical method employing large-eddy simulation to model the turbulence in a Mach 1.19 flow past a cavity with $L/D = 5$.

The present experimental study has been undertaken at the U.S. Air Force Institute of Technology (AFIT) with the intent of gaining a better understanding of the field surrounding a cavity and a store in a compressible flow environment. In each variation, it provides a baseline for comparison to computational results.

Experimental Approach

The AFIT blowdown wind-tunnel facility uses interchangeable convergent–divergent nozzles to generate variable speed flows, depending on the nozzle used. The test section, excluding the cavity, is 6.4 × 6.4 cm. Pressure transducers were used to record the mean pressure in the stagnation chamber and the mean pressure in the freestream of the test section. The resulting pressure ratios yielded Mach numbers of 1.8 and 2.9 for the nozzles used. Flow properties for both nozzles are displayed in Table 1. Figure 1 displays the test section with the Mach 1.8 nozzle in place, wherein flow is from left to right. Endevco 8530C-50 pressure transducers in combination with Endevco Model 4428A signal conditioners were used throughout the experiment, except where noted. Typically, blowdown run times ranged from 10 to 20 s.

The cavity can be seen near the center of Fig. 1b, and the store is shown within its boundaries in Fig. 1c. A pneumatic actuator was affixed to the wind tunnel to extend the store into the supersonic freestream. A bellows and, alternatively, an O-ring encompassing the rod prevented ambient air from entering the test section through the cavity floor, as is evident in Fig. 1d.

Table 1 Flow properties for test conditions for experiments

Property	Mach 1.8	Mach 2.9
T_0, K (°R)	293 (527)	293 (527)
P_0, kPa (psi)	118.6 (17.2)	197.2 (26.8)
T_∞, K (°R)	178 (320)	109 (196)
P_∞, kPa (psi)	20.7 (3.0)	5.5 (0.80)
M_∞	1.8	2.9
u_∞, m/s (ft/s)	481 (1580)	606 (1990)
Re_x (estimated), m^{-1}	5.7×10^5	4.6×10^5

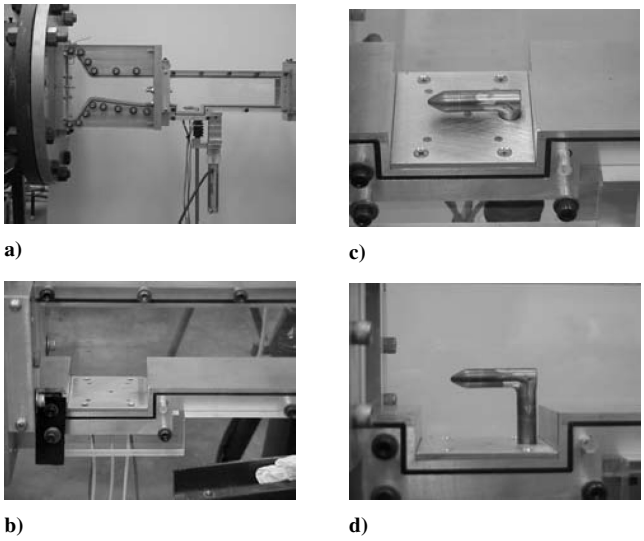

Fig. 1 Test section of experimental apparatus: a) tunnel, Mach 1.8 nozzle, and test section; b) clean cavity model with flush-mounted transducers present; c) cavity with modeled store positioned within the cavity; and d) cavity with simulated store extended into freestream.

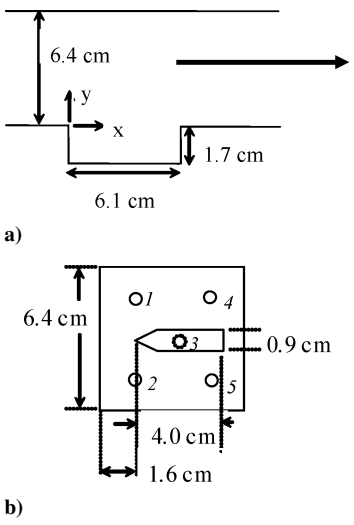

Fig. 2 Schematic of a) side view of cavity and b) top view of store location within cavity with ○, the approximate pressure transducer locations; italicized reference numbers for transducers are given in panel b.

In describing the cavity geometry, the coordinate system used by Zhang and Edwards is followed with x denoting the streamwise direction, y denoting the transverse direction, and z denoting the spanwise direction with $z = 0$ along the tunnel centerline. As shown in Fig. 2, the cavity depth D was 1.7 cm, the cavity length L was 6.1 cm, and its width W was 6.4 cm and spanned the tunnel. The length-to-depth ratio was, thus, 3.6. The store diameter d was 0.9 cm, and its length was 4.0 cm. Five transducers were placed at 1) $x = 1.5$ cm, $z = -1.7$ cm, 2) $x = 1.5$ cm, $z = 1.7$ cm, 3) $x = 3.3$ cm, $z = 0$ cm, 4) $x = 4.6$ cm, $z = -1.7$ cm, and 5) $x = 4.6$ cm and $z = 1.7$ cm. Given the proximity of transducer 3 to the center of the cavity ($x/L = 0.54$ and $z/W = 0$), it is denoted the central transducer (Fig. 2).

Pressure-sensitive paint (PSP) used in this experimental procedure was Innovative Scientific Solutions, Inc. (ISSI), Uni-FIB. Uni-FIB is a single-layer PSP composed of platinum tera (pentafluorophenyl) porphine (PtTFPP) in fluoro/isopropyl/butyl (FIB) binder. One of the key features of this type of paint is very low sensitivity to temperature, which is typically about 0.5% per degree Celsius compared to 5% per psi when utilized in combination with appropriate

lighting and filters. PtTFPP has an excitation spectrum from 380 to 540 nm with a strong peak at 395 nm. The emission spectrum of PtTFPP is from 610 to 720 nm with a peak at 650 nm. For all testing conditions, the PSP was illuminated by an ISSI 2-in.-diam light-emitting diode array at 405 nm. The luminescence from the test area is captured by the camera after passing through a 610-nm Schott glass cutoff filter. The exposure time was optimized for each experimental condition to allow the camera to reach approximately 40% of its saturation level to ensure an adequate signal while preventing saturation. Background images, based on this exposure time, were subtracted from data images to eliminate the effects of camera dark noise and background lighting. All images were collected with a 12-bit Photometrics HQ camera with a 1392×1040 imaging array and a full well capacity of 15,000 photoelectrons.

The experimental procedure began each day with an in situ calibration of the PSP. Because the AFIT blowdown wind-tunnel facility is capable of generating a variety of mean pressures in the test section based on residual pressure within the vacuum tank, the in situ calibration was straightforward. A minimum of eight pressure levels were utilized during calibration that included images of the intensity of the PSP at various pressures, and calibration coefficients were determined.

The windoff image was selected to be close to the mean pressure corresponding to conditions measured for each Mach number. Typically, the reference pressure for the windoff Mach 1.8 case was set near 4.0 psi, whereas that for the Mach 2.9 case was set near 1.0 psi. The images were analyzed by using ISSI spatial mapping software. Following the calibration and windoff image acquisition, the tunnel was activated and windon images were acquired. The data were processed by using the ISSI OMS 3.0 program. The image processing included background subtraction, image alignment, image ratio, conversion to pressure, and resection. The pressure on the cavity floor was verified by the pressure transducers. For a more thorough discussion of the measurement technique, including governing equations, the reader is referred to Bell et al.[12]

The cavity floor mean pressure data were obtained by using an unpainted store with the PSP applied to the cavity floor. The store was manually placed at different positions with respect to the cavity edge ($y = 0$). Positions were below the edge (inside the cavity) at $y = -1$ cm and $y = -0.5$ cm. Positions above the cavity (freestream) included $y = 0.5$ cm. The intensity images were taken directly above the cavity with the Photometrics camera.

When the painted store was used, the preceding procedure was followed, except that two more store positions were added at $y = -0.25$ and 0.25 cm due to the high sensitivity of the pressure on the store in this range. Intensity images were taken with the camera positioned directly above and also at a position of roughly 45 deg off of the nose of the store and slightly below the store. The same procedure and conditions were used for both the Mach 1.8 and the Mach 2.9 nozzles.

Sources of uncertainty for temperature and PSP measurements have been investigated and modeled by Liu et al., who developed a functional relationship between the system components and the elemental error sources.[13] The sensitivity coefficients for the elemental error sources include temperature, illumination, model displacement and deformation, sedimentation, photodegradation, paint calibration, and camera shot noise, as well as errors associated in the measurement of the reference pressure. To determine the overall variance in pressure for a single element, the elemental error is computed and multiplied by its sensitivity coefficient. The total error is computed by summing each elemental error by standard error analysis procedures. For a complete discussion of the error mechanisms, the reader is directed to Ref. 13.

With respect to the high-speed schlieren photography, a standard Z setup was used with mirror focal lengths of 2.04 m each. The light source was an Osram 100-W short-arc mercury lamp 10 mm in diameter and 90 mm long. Images were taken at either 4000 frames per second or at the equipment maximum speed of 16,000 frames per second with a shutter speed of 1/128,000 with a Photron FASCAM-X 1280 PCI camera. Real-time variations in the schlieren images due to the density field changing rapidly were captured.

Results

PSP measurements were performed to gather baseline information on the flow in the proximity of the cavity without the presence of a store. The mean pressure map and pressure coefficients, following the convention used by Stallings and Wilcox[14] for the cavity floor at freestream Mach numbers of 1.8 and 2.9 are shown in Fig. 3. In Fig. 3, the transducers were stationed in the five open circular regions of each image inside the four larger diameter circular regions where the screws holding down the cavity floor were located.

The correspondence of the local PSP measurement to the in situ pressure measurements for the Mach 1.8, clean-cavity case is shown in Table 2. These results were typical. The calibration procedure was conducted at the beginning of every day to account for changes in the luminescence properties of the PSP over time.

For the Mach 1.8 case, the pressure along the span of the farthest downstream portion of the floor is roughly 39% higher than that of the upstream portion of the floor. One interesting characteristic of the Mach 1.8 case is the U-shaped region of lower pressure present upstream of the pressure rise at the trailing edge of the cavity, which indicates a three-dimensional circulation pattern in the region. This phenomenon is not clearly identifiable in the Mach 2.9 flow. Overall, the pressure map appears more uniform for the Mach 2.9 freestream.

These results are generally consistent with the findings of Ref. 14, where static pressure measurements were taken along the spanwise center of cavities for a variety of geometries and flow conditions. One comparison is given in Fig. 4. The PSP data were obtained slightly offset from the centerline because pressure transducer 3 was located on the centerline, whereas the data from Stallings and Wilcox[14] are taken from the centerline of a cavity with $L/D = 4$ and $W/D = 5$ and the data from this experiment are for $L/D = 3.6$ and $W/D = 3.8$. For both sets of data the freestream Mach number was 2.9.

Because the experimental procedure using PSP involves an in situ calibration, short run times, and a clean tunnel, errors due to sedimentation and photodegradation are minimal. Of the remaining sources of error, temperature, camera shot noise, accuracy of the paint calibration curve, and consistency of illumination are identified as the major sources of uncertainty. Near the cavity floor, the flow is subsonic, and the recovery temperature is approaching the stagnation temperature of the flow. The cavity floor is constructed by using metal, which has a high thermal conductivity. This yields a near isothermal boundary condition. This combination serves to minimize any temperature defects or gradients on the cavity floor. To verify the assumption of negligible temperature effects, during one of the Mach 2.9 runs, a pressure transducer on the cavity floor was replaced with a thermocouple, and the difference from ambient was no more than a few degrees Kelvin. The effect of model displacement during PSP was also minimal because the floor was both flat and rigidly attached to the tunnel. The approximate relative error inherent to PSP with the transducers is listed in Table 3.

Table 2 Correlation of transducer and PSP pressure readings for Mach 1.8 freestream clean-cavity case

Transducer number	Pressure, psia		Difference, psi
	Transducer	PSP	
1	4.18	4.23	0.05
2	4.26	4.25	−0.01
3	4.03	4.04	0.01
4	3.99	4.02	0.03
5	3.94	3.99	0.05

Table 3 Estimate of pressure error due to various sources for cavity by using PSP

M	Shot noise	T	P_{ref}	Calibration	Displacement	Total error, psi
1.8	0.10	0.05	0.02	0.02	.01	0.24
2.9	0.03	0.01	0.02	0.02	.01	0.07

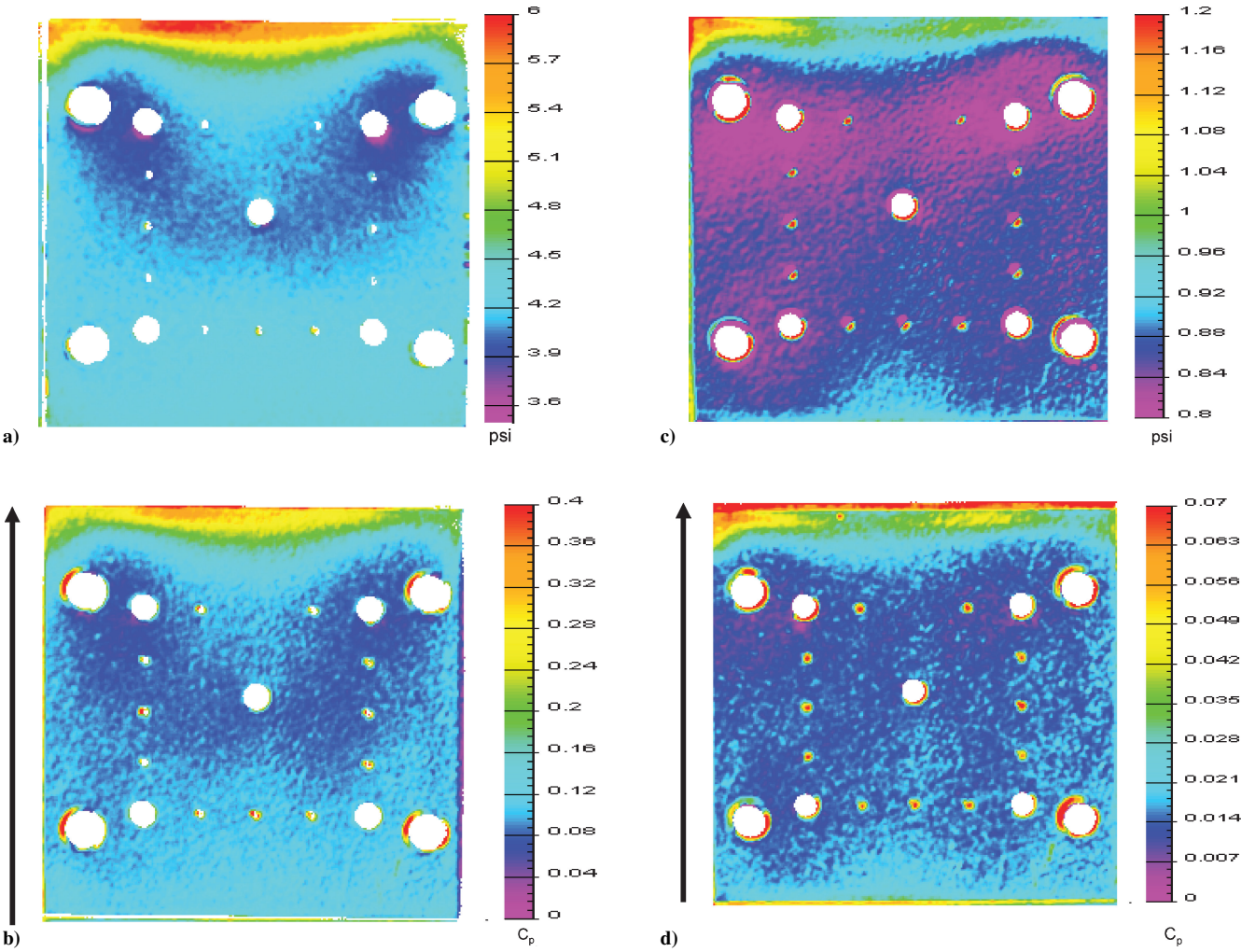

Fig. 3 PSP measurements of cavity floor with no store present: a) Mach 1.8 mean pressure, b) Mach 1.8 C_p, c) Mach 2.9 mean pressure, and d) Mach 2.9 C_p; flow direction is from bottom to top for each image, as indicated by arrows.

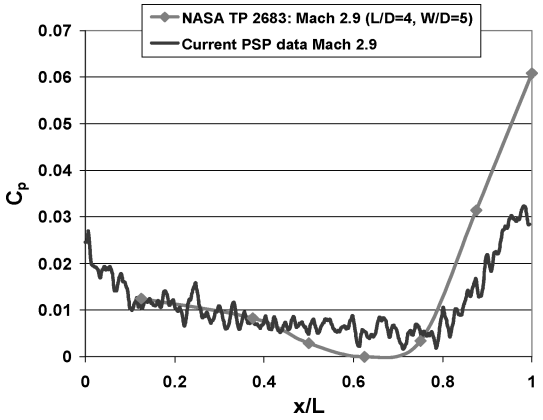

Fig. 4 Pressure coefficient comparison of Mach 2.9, clean-cavity PSP data and pressure tap data for cavity of similar dimensions, operated under similar conditions.[14]

Pressure data were acquired by each Endevco transducer at 100 kHz. The data were averaged in bins of 512 points, and 196,608 data points were used. The temporal pressure fluctuations normalized by the mean pressure are shown in Fig. 5a for the central transducer (no. 3) with no store for Mach 1.8 and 2.9 test conditions. The corresponding power spectra are given in Fig. 5b. The Mach 1.8 condition yielded a strong peak near 7 kHz, with a weaker subharmonic peak located near 14 kHz. When the approach of Rockwell and Naudascher[3] is used, the $n = 5$ Rossiter mode under the test conditions equates to a frequency of 7.0 kHz. For one point of comparison, Zhang and Edwards report a peak at roughly 6.0 kHz at Mach 1.5 in a cavity with $L/D = 4$, where D was 1.5 cm as opposed to 1.7 cm in the present study. Note that Fig. 5 is given in terms of power spectral density computed from the voltage output of the signal conditioner and that the frequency is plotted in a linear format.

Figure 5b shows the absence of a distinct peak in the spectra taken from the cavity floor for a freestream Mach number of 2.9. This result was in stark contrast to the Mach 1.8 results. To rule out the possibility the lower mean pressure values corresponding to the Mach 2.9 freestream were responsible for the lack of a coherent spectral peak, the 50-psia Endevco transducers in locations 3 and 4 were replaced with 15-psia gauges, thereby increasing the signal-to-noise ratio by a factor of three, which resulted in comparable signal-to-noise ratios for the Mach 1.8 and 2.9 cases. Despite the higher fidelity of the transducers, the spectral content for the Mach 2.9 case was virtually unchanged from the data presented in Fig. 5.

Based on the uninterrupted section length upstream of the cavity and freestream conditions, the Reynolds number Re is estimated to be 4×10^5, which is transitional. As a side note, for the Mach 1.8 test condition, a Reynolds number of 6×10^5 was calculated. As noted earlier, Heller et al.[7] showed that the upstream boundary-layer state influences the development of cavity tones for a Mach 3 freestream, but was of less consequence for lower freestream Mach number values. The results presented here are consistent overall with those findings, though in actuality the Reynolds number in the current

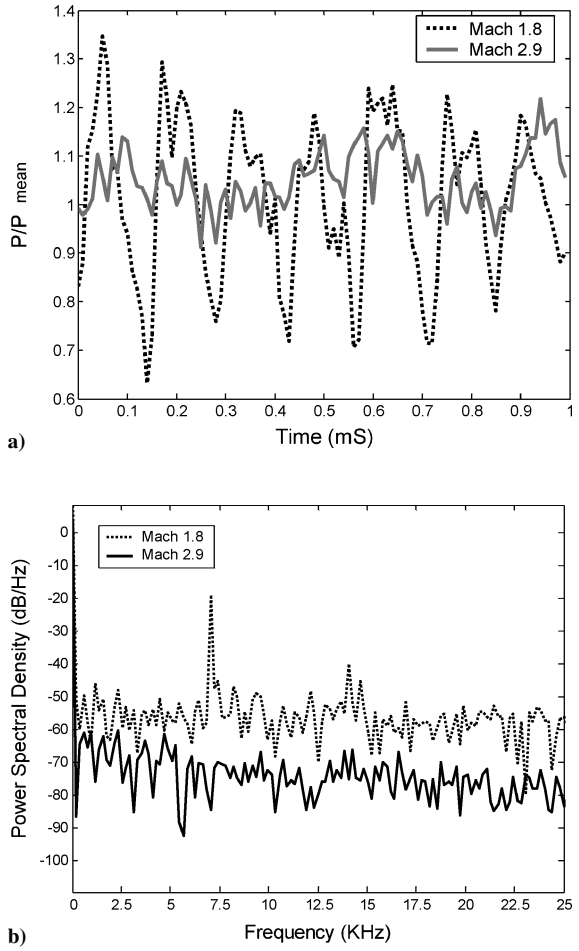

Fig. 5 Temporal pressure data for the central transducer (no. 3) located within the cavity floor: a) normalized time signals and b) power spectra.

experiment is relatively close to that characterized as laminar by Heller et al.

Sequences of successive schlieren images of the clean cavity were analyzed to characterize the flow properties. The images were acquired at 16,000 frames per second with a shutter speed of 1 μs. In the Mach 1.8 flow, views of the whipping flow and widening shear layer that are commonly associated with flow over a cavity were captured. A sample is shown in Fig. 6. A more complete set of images is given by Bjorge.[15] Using the convective velocity predicted by Murray and Elliott, one would expect a structure to convect 1.7 cm (0.68 in., which is $0.28L$) downstream per frame. This corresponds well qualitatively to the results shown in Fig. 6, where a single structure is subjectively tracked from approximately $0.2L$ to $0.8L$ in the course of three successive frames, as noted by the carats above those images.

When the Mach number was increased to 2.9, it became nearly impossible to correlate flow structures qualitatively from frame to frame in any meaningful way, as can be seen in Fig. 7. Whereas the freestream velocity was somewhat higher, the predicted movement is 2.2 cm (0.85 in., which is $0.35L$) per frame, which falls within the range that could be captured by the camera in real time. The whipping motion clearly identified for Mach 1.8 was not present. The most likely explanation is that the structures within the free shear layer decrease in spanwise coherence. As a result, the optical averaging inherent to schlieren photography obfuscates the convection and development of individual density waves. That said, there are some interesting features of Fig. 7 that should be noted. For example, an individual shock emanating from a particularly strong flow structure within the shear layer is evident in the third image. Also note that the shock structure formed at the trailing edge of the cavity is remarkably similar in the first and fourth frames.

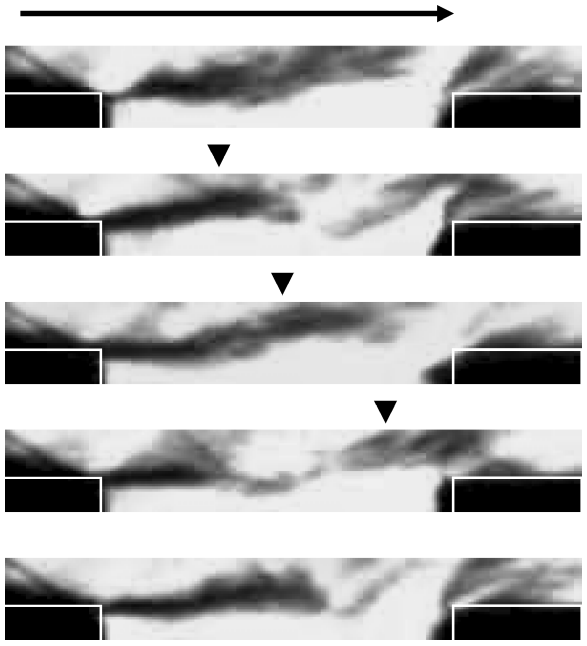

Fig. 6 Five successive schlieren images separated by 6.25*e*−5 s (frame rate of 16,000 frames per second) characterizing shear layer for Mach 1.8 flow; in this side view, flow direction is left to right, as indicated by arrow; carats indicate relative *x* position of flow structure at its approximate convective velocity; and white lines indicate cavity geometry (cavity floor not visible).

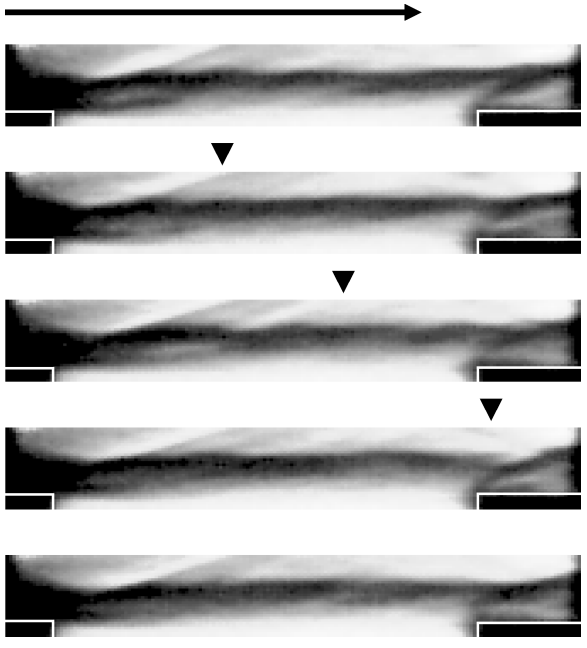

Fig. 7 Five successive schlieren images separated by 6.25*e*−5 s (frame rate of 16,000 frames per second) characterizing shear layer for Mach 1.8 flow; in this side view, flow direction is left to right, indicated by arrow; carats indicate relative *x* position of possible flow structure at its approximate convective velocity, and white lines indicate cavity geometry (cavity floor not visible).

The effect of the store on the frequency spectra measured by transducer 3 for Mach 1.8 is shown in Fig. 8. As the store placement was changed from inside the cavity to locations nearer to, and finally within, the freestream, the magnitude of the resonant peak was diminished. With the store positioned within the cavity, the spectrum is similar to that of the cavity without the store present. There is a peak at 7.0 kHz, though its amplitude has been reduced by about 17 dB compared to the clean cavity. Likewise, a subharmonic is present at

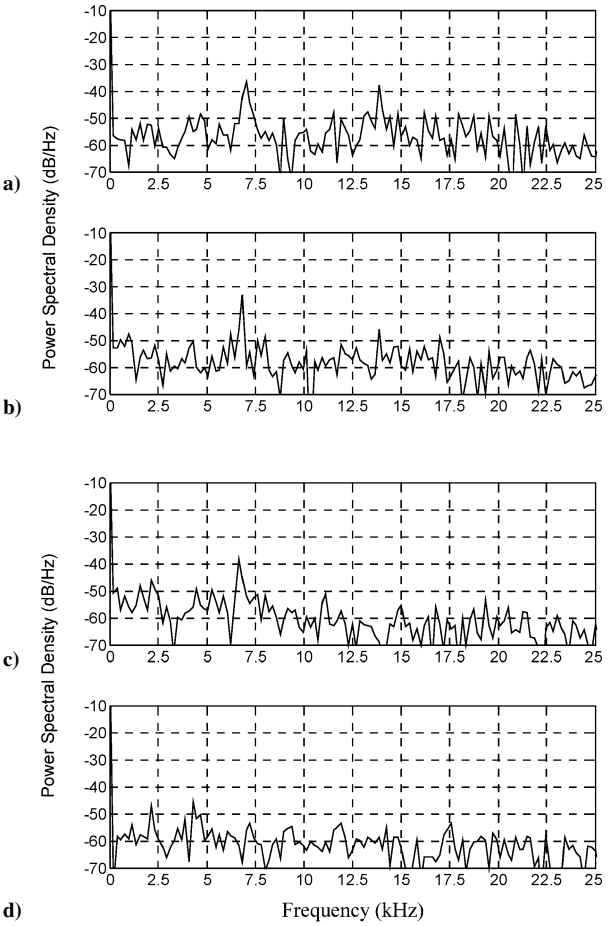

Fig. 8 Power spectra taken from central transducer for stationary store at four different vertical positions: a) $y = -1.0$, b) -0.5, c) 0, and d) 0.5 cm for freestream Mach number of 1.8.

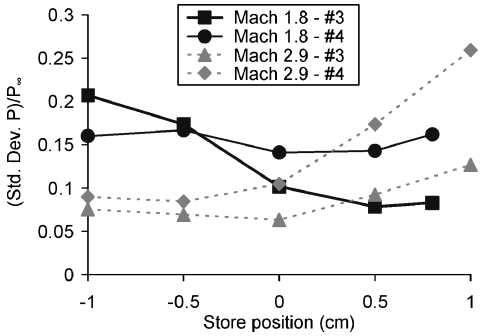

Fig. 9 Standard deviation of pressure from central transducer and transducer near trailing edge of cavity as function of store location for Mach = 1.8 and 2.9; $y = 0$ location along plane of cavity lip.

14 kHz. With the store positioned at -0.5 cm, the peak in the spectra shifted from 7.0 to 6.8 kHz and increased slightly, whereas the level of the subharmonic dropped slightly. With the store position increased to $y = 0$, the peak frequency was 6.6 kHz, and the level dropped slightly. With the store positioned at $y = 0.50$ cm, the tone was indistinguishable from background noise. The periodic pressure fluctuations diminish as the store moves from inside the cavity, through the shear layer, and into the freesteam.

Analysis of the Mach 2.9 frequency spectra for various store positions yielded similar results to the clean-cavity conditions shown in Fig. 4 in that no clearly identifiable resonant peaks were observed.

Figure 9 shows the trends of the standard deviation of the central transducer 3 and transducer 4, located near the rear wall of the cavity for both freestream Mach numbers. Here, fluctuating pressure values are normalized by their respective freestream pressure. The first noteworthy difference is the overall trend of the Mach 1.8 vs the Mach 2.9 cases. The central transducer for the Mach 1.8 condition reveals an overall decrease in the standard deviation as the store is moved from inside the cavity into the freesteam, whereas transducer 4 was nearly constant. This is consistent with the frequency spectra data. The Mach 2.9 case has the opposite trend as the standard deviation increases as the store is extended into the freestream. No comparisons can be made with the frequency spectra data because a resonant peak was not observed at any store location for the Mach 2.9 condition. However, the data in Fig. 9 do reveal the influence the store has on the fluctuation of the pressure on the cavity floor for that case. One possible explanation is that as the store is moved into the freestream, it may divert more energy from the supersonic flow into the shear layer and, subsequently, into the subsonic cavity region, generating greater pressure fluctuations. The increased level of fluctuations is particularly pronounced for transducer 4, located closer to the rear wall.

A time-averaged schlieren photographs of the cavity with the store present is given in Fig. 10. The images were acquired with an

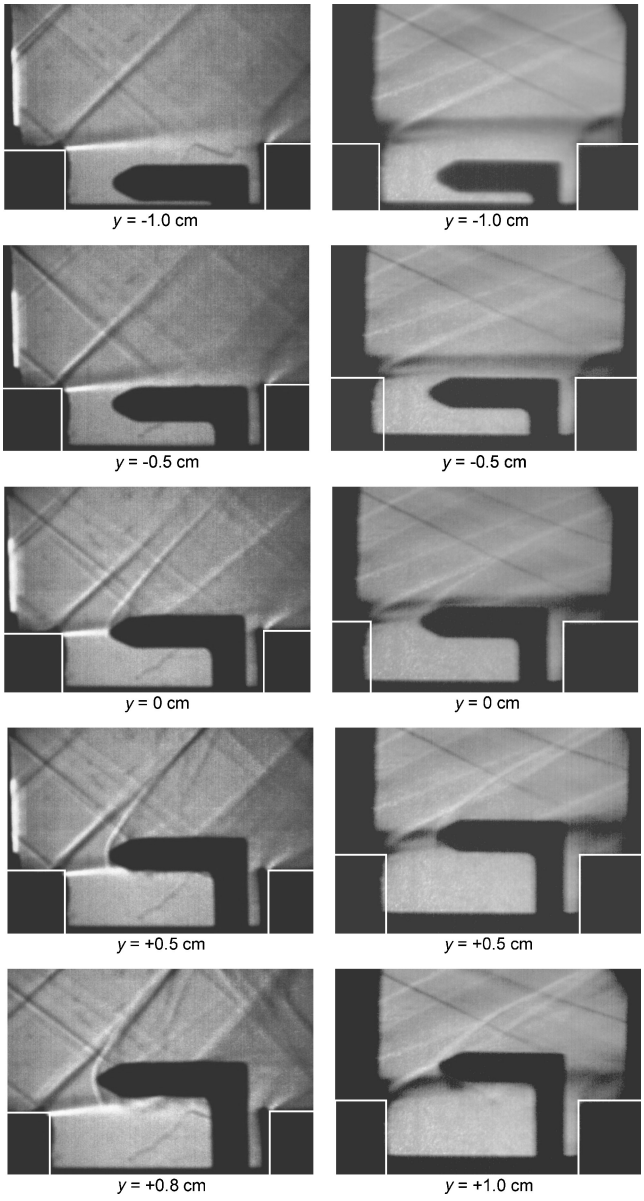

Fig. 10 Time-averaged schlieren photographs of flow with stationary store at five y locations: the left column shows images for Mach 1.8 freestream and the right column shows images for Mach 2.9 freestream; exposure time 0.001 s, white lines indicate cavity geometry.

exposure time of 1 ms. With the store positioned completely within the cavity, there is no visual effect from the store on the creation of the shear layer as the flow interacts with the cavity. Note that the images were obtained at different times, and subtle differences in lighting between the Mach 1.8 and 2.9 images are due to small variations in the setup of the schlieren equipment. Notable features of the unimpeded flow are the shock wave at the leading edge, the free shear layer, and the shock impinging on the downstream portion of the cavity. It also appears that an expansion fan is located just downstream of the cavity. These observations are consistent with published results.

As the store begins to enter the shear layer at the $y = 0$ position, the store dramatically changes the flow properties. The most obvious change is the shock wave that forms on the nose of the store as it enters the supersonic flow. A small expansion fan is attached to the stores upper surface as the conical nose transitions to the cylindrical body. One difference visible between the Mach 1.8 and 2.9 cases is that the impingement shock on the rear of the cavity is disrupted in the Mach 2.9 flow, but is still visible in the Mach 1.8 flow.

At store position $y = +0.5$ cm, the nose of the store is slightly above the free shear layer, and a shock wave appears to be forming on the underside of the store toward the cavity, as well as continuing into the freesteam. Image analysis of the Mach 1.8 case indicated that the angle of the shear layer, defined by the transition from bright to dark, with respect to the freestream increased from 4.5 deg for a store placement of $y = -1.0$ cm to 7.4 deg for $y = +0.8$ cm. A similar general trend can be seen for the Mach 2.9 case. It is unclear how much of this shift could be due to the rear support of the modeled store. More details of the analysis of the shift in the free shear layer are contained in Ref. 13.

The small difference in the location indicated for the last row of images arises because when the store was positioned at $y = +1.0$ cm in the Mach 1.8 flow, the flow was choked. This was not an issue for the Mach 2.9 condition. At this y location, the store has exited the cavity, except for the attachment rod. Notably, the shock ends when it hits the shear layer at the cavity. One would expect an expansion fan to be reflected back toward the store. Indeed, on close observation, a subtle pattern can be identified for freestream Mach numbers of both 1.8 and 2.9. However, it is impossible to state definitively that this is the case, in part due to the spanwise optical averaging inherent in Schlieren photography.

The strong density gradients responsible for the bright and dark regions of Fig. 10 suggest the y location where a released store is likely to undergo great variations in surface pressure between its upper and lower surfaces as it moves out of the cavity into a supersonic freestream. This is corroborated by the literature and by analysis of the PSP data.

PSP data were acquired on the cavity floor with a store in place for each Mach number and are shown in Fig. 11. The mean pressure on the cavity floor with the store in place displays a similar pattern as those taken without the store, with the exception of a slight overall increase in mean pressure. As the store is moved out of the cavity, the mean pressure continues to increase. At positions $x = 5$ cm and $z = 1.3$ cm, the pressures were compared for the various store heights.

For the Mach 1.8 freestream, the pressure increased from 4.3 to 5.3 psi, roughly a 25% increase. For the Mach 2.9 freestream, the pressure increased from 0.8 to 1.3 psi, roughly a 60% increase. This is plausibly a result of the shock that is formed at the nose of the store. Note that the apparent low-pressure zones in the $y = -0.5$ cm position for the Mach 2.9 condition are concurrent with shadows cast by the store. As such, these regions are likely the result of experimental bias for that isolated case.

PSP was also utilized to measure the pressure distribution on the store for both conditions. Figure 12 combines two separate views of the store. The top (freestream side) view of the store is shown in the upper portions of Fig. 12, whereas a perspective view, primarily taken from the side of the store, is shown in the lower portion of Fig. 12. In each case, the store was positioned at different y locations, as noted. Note that the angle of attack of the store was set to zero for each image. The apparent angle in the side is due only to the camera

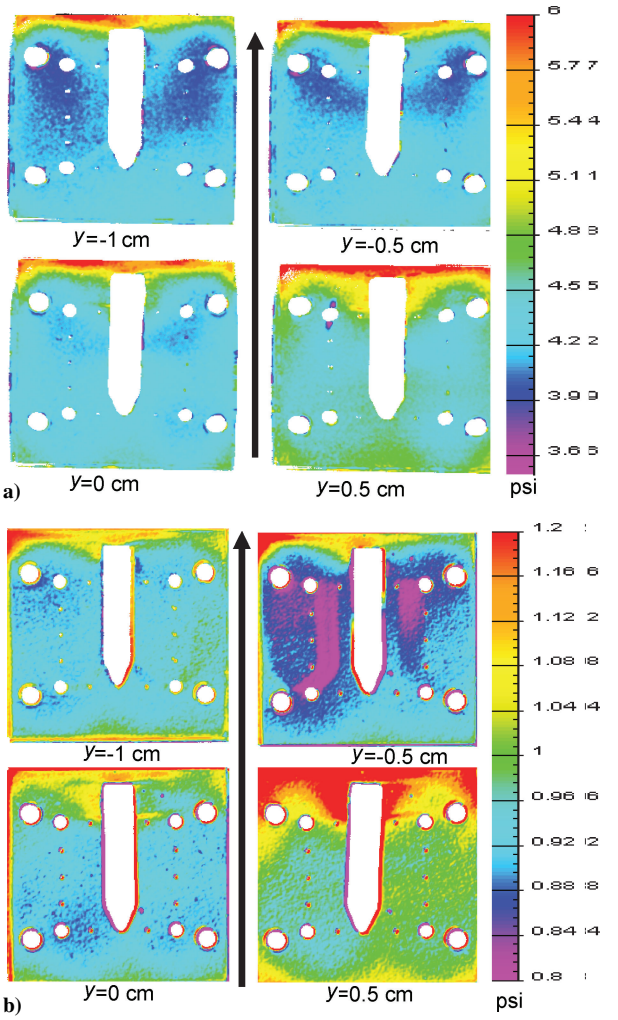

Fig. 11 Effect of store position on mean pressure on cavity floor viewed from above cavity floor, where $y = 0$ position corresponds to store positioned at cavity edge for: a) Mach 1.8 and b) Mach 2.9; flow direction from bottom to top, indicated by arrows.

angle, and the images were not reoriented to maintain information relating to the camera perspective.

The PSP measurements on the store showed some common trends for both freestream Mach number cases studied. At the $y = -0.5$ position, the store is within the cavity, and its surface pressure is nearly uniform. As the y position of the store was increased, a distinctive pattern was evident for both Mach number conditions. Pressure rose on the nose of the store in the shear layer and moved into the freestream. There is an area of lower pressure on the upper surface of the cylindrical body just aft of the nose, presumably due to the expansion fan that was visible in the schlieren images. On the lower surface of the nose of the store, a small region of lower pressure appeared when the store was at the $y = 0$ position. This low-pressure region remains intact when the store is moved toward the freestream. This is likely related to the shift in shear-layer trajectory due to store placement. This corresponds well with observations of the schlieren images. The discontinuities near the trailing edge of the store for the Mach 2.9 side view were due to lubricant contamination. Note that changes in the recovery temperature on the surface of the store generally adds error due to temperature sensitivity of the paint. However, given the relative independence of paint from temperature effects, this is deemed a minor contributor in this instance.

In an ideal setting, one could utilize the surface pressure data acquired via PSP to compute highly accurate lift, drag, and moment coefficients. The pressure maps acquired from the side views in this study provide sufficient information to compute these values with sufficient accuracy to identify trends in these coefficients as a function of store position. The pressure data were interactively

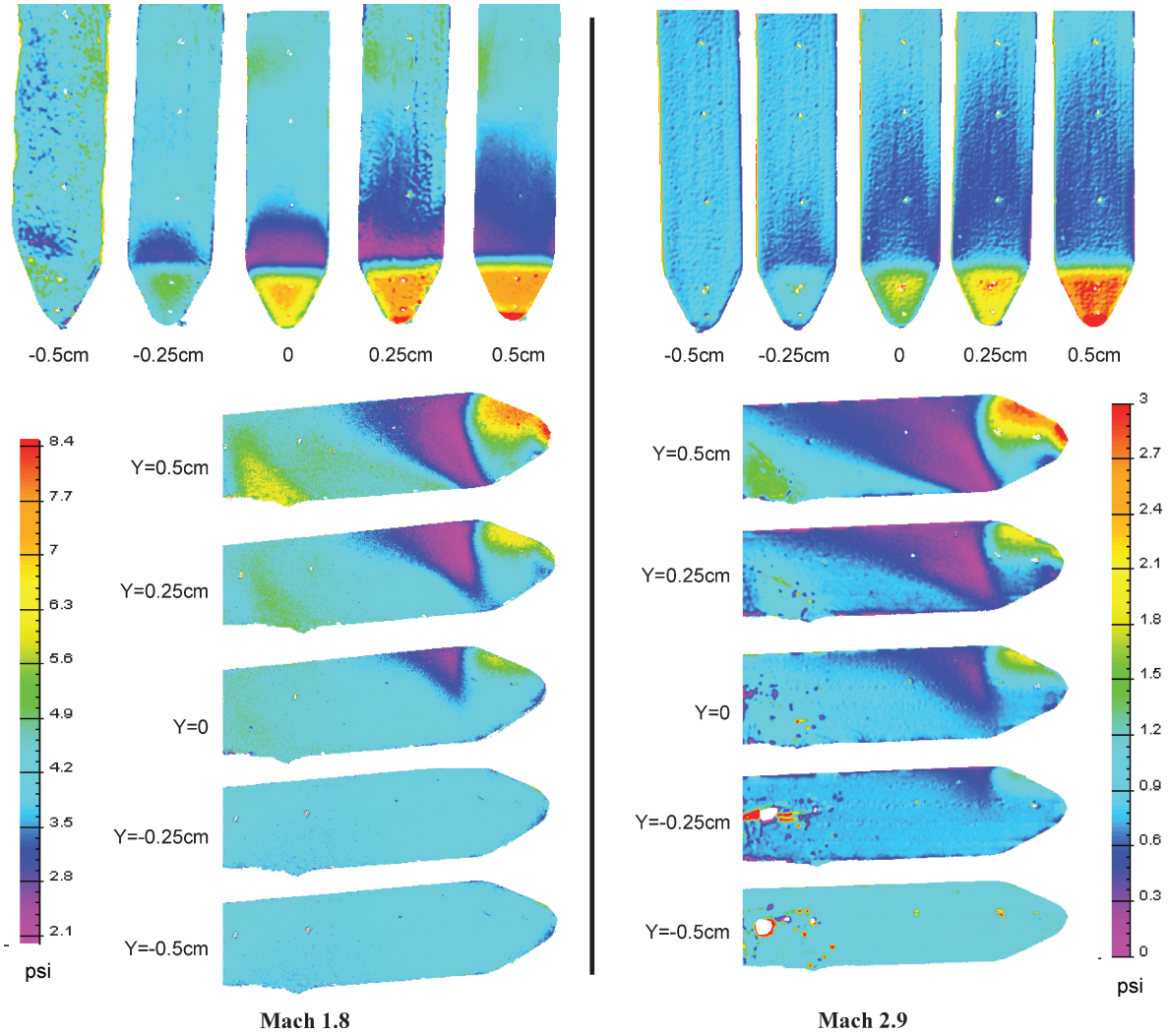

Fig. 12 Effect of store position, relative to cavity floor, on mean surface pressure of store, with lower images taken with camera located on a plane roughly even with cavity floor and viewing from slightly upstream of the store; actual angle of attack of store is 0 deg.

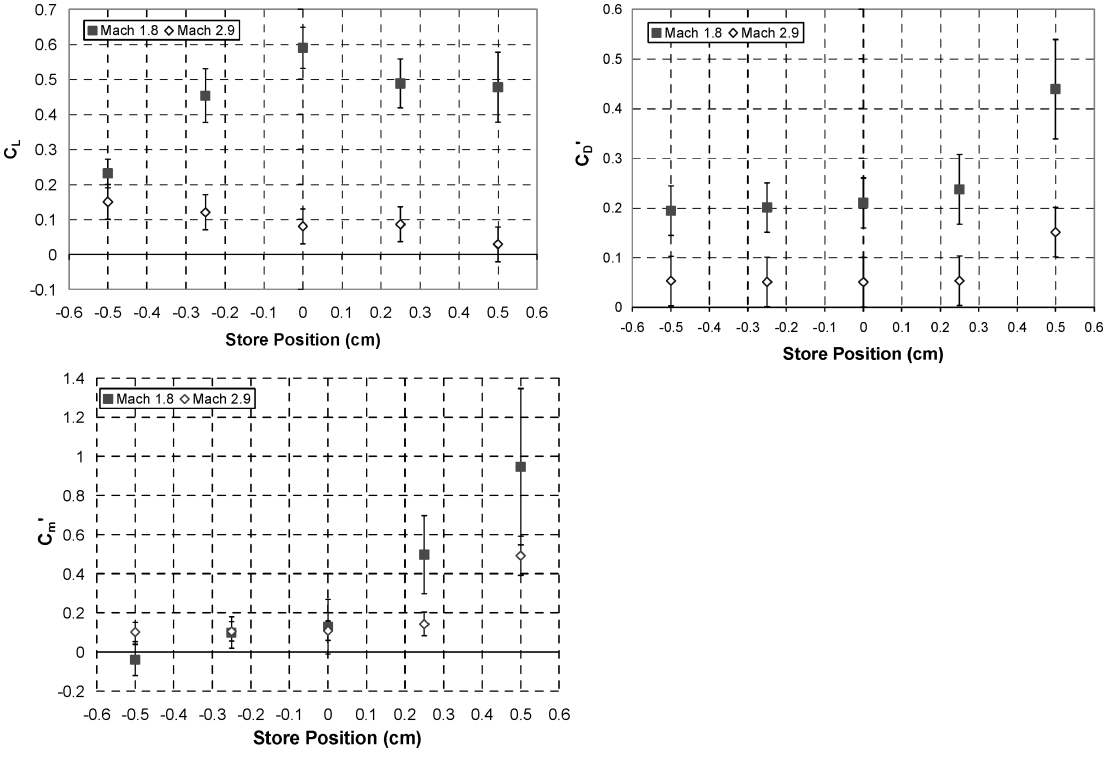

Fig. 13 Lift, drag, and moment coefficients calculated from PSP data for various store locations.

mapped onto the surface of the model and subsequently integrated using the ISSI software programs ProField and ProImage. Because the camera position was not changed for each image acquisition, variations in position of the store as the images were recorded made each alignment slightly different. To complete a computation of the lift coefficient, lateral symmetry was assumed. Furthermore, error bars based on a combination of errors due to pressure measurements as discussed earlier and, in addition, due to mapping the two-dimensional image plane onto a three-dimensional surface are provided.

The computation of a drag coefficient and moment coefficient, taken about the longitudinal center of the store, is further hindered by a lack of information on the pressure at the base of the model. Therefore, the coefficients are given as C'_D and C'_m in recognition that this contribution could be significant, particularly for the drag coefficient. The computed values of each coefficient are given in Fig. 13.

Several conventions mandated by the cavity-based coordinate system used here should be noted. These coefficients were calculated based on area normalization equal to the length of the store (4.0 cm) multiplied by its diameter (0.9 cm), and the diameter was used for the reference length used to calculate the pitching moment coefficient. The sign convention in Fig. 13 was taken such that a positive lift coefficient is indicative of a force that would act to move the store away from the cavity floor. A positive moment coefficient indicates a moment that would act to bring the nose toward the cavity floor and rotate the tail away from the cavity floor. The moment coefficient given in Fig. 13 was taken about the longitudinal center of the store.

The measured coefficients for the Mach 1.8 case were typically larger than their Mach 2.9 counterparts. This could be a result of the changes in the thickness of the free shear layer due to compressibility. Among the simplest features of Fig. 13 to interpret is that the drag coefficient tends to increase as the store is positioned closer to the freestream, which is an expected trend. It is possible that the values for the Mach 2.9 case lag those of the Mach 1.8 case as y is increased, in part due to increased deflection of the shear layer at the higher speed. At the lowest store position, it is likely that the lack of a correction for base drag is the source of a positive value for C'_D.

An interpretation of the trend in the lift is considerably less tractable. For the Mach 1.8 freestream, the lift coefficient appears to increase to a peak of about 0.6 at $y = 0$, then decrease once the model is extended into the freestream. In contrast, the Mach 2.9 case showed little change in C_L due to y position.

The moment coefficient C'_m measurement from PSP shows a similar trend for both Mach numbers in that there is a positive increase in its value as the y position is increased and the model enters the freestream. This trend occurs at a slightly lower y position for the Mach 1.8 case than for the Mach 2.9 case.

Additional insight can be gleaned from flow visualization of a dynamic simulated separation event. A qualitative analysis of the flow about a moving store was performed using high-speed schlieren photography. A pneumatic actuator rapidly moved the store from within the cavity into the freestream. On activation, the store moved from within the cavity into the freestream in about 15 ms. The images shown in Fig. 14 correspond to the Mach 1.8 freestream, whereas those for the Mach 2.9 case are shown in Fig. 15. Slight differences in the experimental setup for the two cases prevented a 1:1 correspondence in the field of view. In Fig. 14, the interaction of the free shear layer and the store can be seen even in the first frame, which corresponds to a value for y of just under -0.25 cm. In the Mach 2.9 images, this interaction did not typically occur until y increased above -0.25 cm.

The images in Fig. 14 show some interesting qualitative features for the two unsteady events, namely, the whipping motion of the free shear layer and the linear store motion. Note that the even the first image, corresponding to the store location fully within the cavity, shows two small dark lines near the shoulder of the store. In the second image of the sequence, the dark region of the image near the shoulder is larger, as one might expect, whereas in the third image, the dark attachment region is located farther downstream on the store. Note that on reviewing images of dozens of release events,

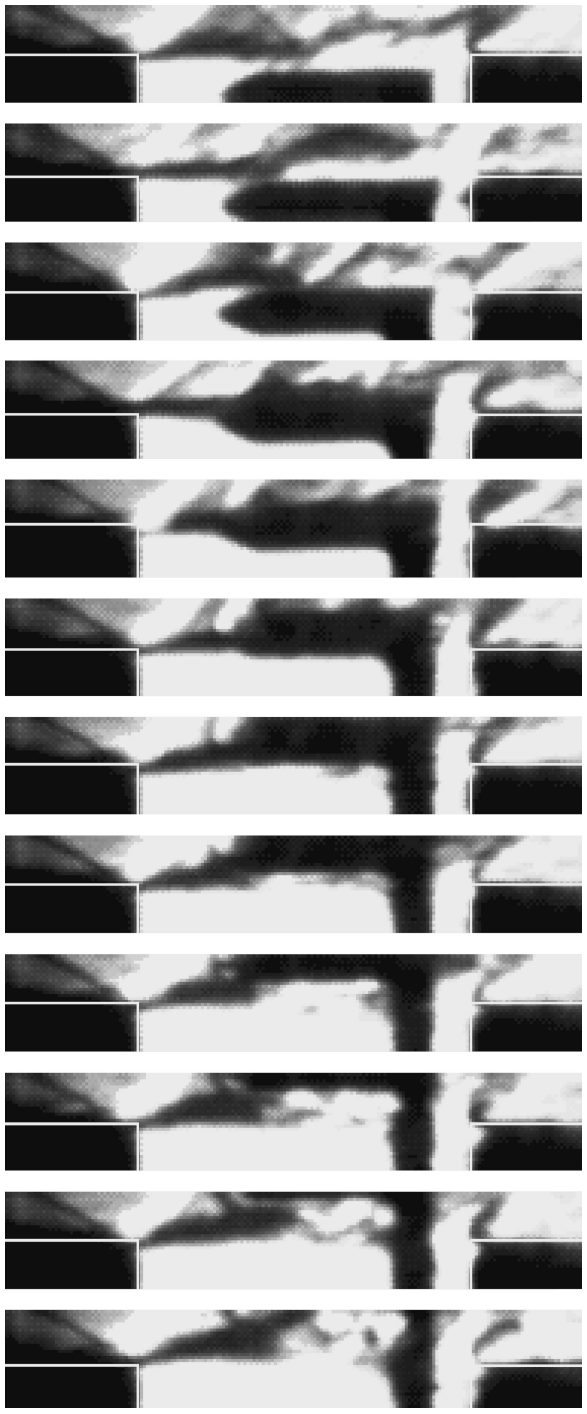

Fig. 14 Side view of sequence of 12 images of simulated store moving into Mach 1.8 freestream, the sequence beginning with the store within the cavity (top) and passing through the free shear layer to the freestream; photographs are separated by 1.25×10^{-3} s and are essentially uncorrelated in time, apart from the store motion, exposure time for each image being 1×10^{-6} s and white lines indicating the cavity geometry.

there was no clearly discernable pattern in the way the shear layer initially interacted with the store. This suggests that the pressure field due to the motion of the shear layer generates a high level of difficulty in predicting the initial condition of the store. Naturally, a minor change in its initial trajectory caused by the initial interaction of the shear layer with the store could potentially influence the store's exit trajectory.

Additionally, note that the images suggest that the store motion could influence the trajectory of the free shear layer. Specifically, in the last few images, the trajectory of the shear layer is slightly more

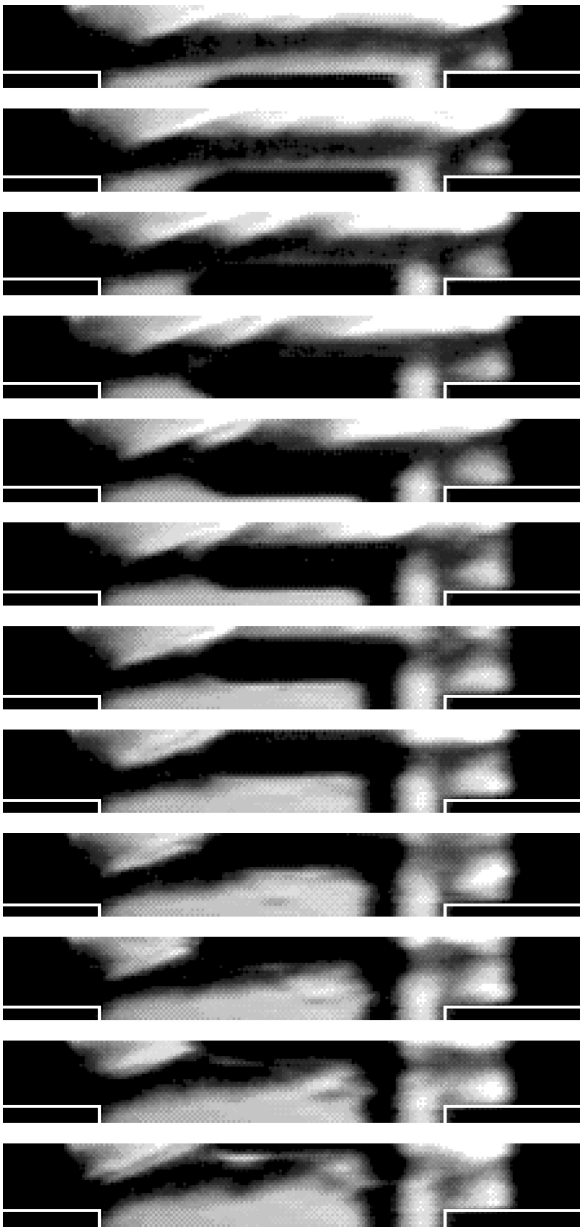

Fig. 15 Side view of sequence of 12 images of simulated store moving into Mach 2.9 freestream, the sequence beginning with the store within the cavity (top) and passing through the free shear layer to the freestream; photographs are separated by 1.25×10^{-3} s and are essentially uncorrelated in time, apart from the store motion, exposure time for each image being 1×10^{-6} s and white lines indicating the cavity geometry.

toward the freestream. This could be of consequence in applications where two or more stores are released in sequence. However, note that the support rod attached to the store model cannot be ruled out as a strong source for this alteration in shear layer trajectory.

In the sequence for the Mach 2.9 case shown in Fig. 15, there was considerably less variability in the shear layer and how it interacted with the moving store. On the other hand, there is more evidence of the free shear layer rising up with the store and its support shown in Fig. 15. As the store exits the cavity, the shear layer appears to impinge on the store at the same location, even though the store continues to move out of the shear layer.

Summary

The flow characteristics over a fixed geometry cavity ($L/D = 3.6$) with freestream Mach numbers of 1.8 and 2.9 were analyzed by using fast-response pressure transducers, PSP, and high-speed schlieren photography. These measurements were carried out for both a clean cavity and for a cavity containing a modeled store to better capture the flow physics corresponding to a weapons release.

Schlieren photography of the clean cavity indicated that the three dimensionality of the flow increased at higher Mach numbers, which is consistent with the literature. This observation was reenforced by analysis of the frequency spectra measured by transducers located on the cavity floor, which indicated the absence of a resonant peak when the freestream was Mach 2.9. High-speed schlieren images for both a stationary and a rapidly translating store were also captured for both freestream conditions. In general, the visualized density gradients indicated strong fluctuations in the instantaneous pressure field, which could affect store trajectory.

The presence of a store in proximity to the cavity produced some interesting changes in the mean and fluctuating pressure on the cavity floor. In the Mach 1.8 flow, the resonant tones associated with cavity flow were present when the store was within the cavity, but were eliminated when the store was placed within the free shear layer ($y \geq 0$). For both the Mach 1.8 and the March 2.9 freestream, the mean pressure levels on the cavity floor increased as the store location was shifted from within the cavity ($y < 0$) to locations outside the cavity ($y > 0$). On the other hand, the standard deviation of the pressure on the cavity floor showed opposing trends, decreasing for Mach 1.8 and increasing for Mach 2.9 as y was increased.

PSP applied to the modeled store provided global mean pressure measurements. With reference to Fig. 12, the overall pressure on the freestream side of the nose of the store is higher than on the cavity side. Aft of the nose, the trend is opposite because pressures are higher on the cavity side of the straight section of the store than on the freestream side of the store. Schlieren images of a stationary store showed that the shear layer was disrupted by the store when it was placed at or outside of the free shear layer. An analysis of the images indicates that the shear layer shifts outward toward the store when the y location of the store is greater than zero.

When the surface pressure data gathered from PSP is used, force and moment coefficients are computed for each store position by integrating over the surface of the store. Despite limitations due to the lack of data at the base of the store and accuracy limits due to spatial mapping, a number of clear trends were identified. In general, both the drag coefficient and the moment coefficient increased as the store position was shifted toward the freestream. The lift coefficient was positive for each measurement, which is generally consistent with the faster moving air on the freestream side of the store, but it exhibited significantly different values for the two Mach number cases studied.

Acknowledgments

The authors thank A. Pitts and J. Anderson for their technical expertise, which was instrumental in the execution of this experiment. The authors also thank the reviewers for their valuable comments and suggestions, which led to substantial improvements in this paper. The authors acknowledge the guidance and support of J. Anttonen of the U.S. Air Force Research Laboratory (AFRL)/Munitions Directorate and M. Stanek and J. Grove of AFRL/VA. The views expressed in this article are those of the author and do not reflect the official policy or position of the United States Air Force, Department of Defense, or the U.S. Government.

References

[1]Cattafesta, L., Williams, D., Rowley, C., and Alvi, F., "Review of Active Control of Flow-Induced Cavity Resonance," AIAA Paper 2003-3567, June 2003.

[2]Stanek, M. J., Raman, G., Kibens, V., Ross, J. A., Odedra, J., and Peto, J. W., "Suppression of Cavity Resonance Using High Frequency Forcing—The Characteristic Signature of Effective Devices," AIAA Paper 2001-2128, May 2001.

[3]Rockwell, D., and Naudascher, E., "Review—Self-Sustaining Oscillations of Flow Past Cavities," *Journal of Fluids Engineering*, Vol. 100, No. 2, 1978, pp. 152–165.

[4]Zhang, X., and Edwards, J. A., "An Investigation of Supersonic Oscillatory Cavity Flows Driven by Thick Shear Layers," *Aeronautical Journal*, No. 940, Dec. 1990, pp. 355–364.

[5]Murray, R., and Elliott, G., "Characteristics of the Compressible Shear Layer over a Cavity," *AIAA Journal*, Vol. 39, No. 5, 2001, pp. 846–856.

[6]Unalmis, O. H., Clemens, N. T., and Dolling, D. S., "Experimental Study of Shear-Layer/Acoustics Coupling in Mach 5 Cavity Flow," *Journal of Aircraft*, Vol. 39, No. 2, 2001, pp. 242–252.

[7]Heller, H. H., Holmes, D. G., and Covert, E. E, "Flow Induced Pressure Oscillations In Shallow Cavities," *Journal of Sound and Vibration*, Vol. 18, No. 4, 1971, pp. 545–553.

[8]Shalaev, V. I., Fedorov, A. V., and Malmuth, N. D., "Dynamics of Slender Bodies Separating from Rectangular Cavities," *AIAA Journal*, Vol. 40, No. 3, 2002, pp. 517–525.

[9]Mosbarger, N. A., and King, P. I., "Time-Dependent Supersonic Separation of Tangent Bodies," *Journal of Aircraft*, Vol. 33, No. 5, 1996, pp. 938–949.

[10]Baysal, O., Fouladi, K., Leung, R., and Sheftic, J., "Interference Flows Past Cylinder–Fin–Sting–Cavity Assemblies," *Journal of Aircraft*, Vol. 29, No. 2, 1992, pp. 194–202.

[11]Rizetta, D. P., and Visbal, M. R., "Large-Eddy Simulation of Supersonic Cavity Flowfields Including Flow Control," *AIAA Journal*, Vol. 41, No. 8, 2003, pp. 1452–1462.

[12]Bell, J. H., Schairer, E. T., Hand, L. A., and Mehta, R., "Surface Pressure Measurements Using Luminescent Coating," *Annual Review of Fluid Mechanics*, Vol. 33, 2001, pp. 155–206.

[13]Liu, T., Guille, M., and Sullivan, J. P., "Accuracy of Pressure Sensitive Paint," *AIAA Journal*, Vol. 39, No. 1, 2001, pp. 103–112.

[14]Stallings, R. L., and Wilcox, F. J., "Experimental Cavity Pressure Distributions at Supersonic Speeds," NASA TP 2683, June 1987.

[15]Bjorge, S., "Flow Around an Object Projected into a Supersonic Freestream," M.S. Thesis, Dept. of Aeronautics and Astronautics, U.S. Air Force Inst. of Technology, Wright–Patterson AFB, OH, March 2004.

R. Lucht
Associate Editor

Color reproductions courtesy of U.S. Air Force Institute of Technology.